Cylindrical Optic Figuring & Dwell Time Optimization

Eugene Waluschka
NASA Goddard Space Flight Center
Optics Branch/551.0
Greenbelt, Maryland 20771

ABSTRACT

Grazing incidence x-ray telescopes consist of surfaces which are nearly cylindrical in shape. The abrasive figuring of these surfaces is accomplished by moving a grinding tool along a helical path on this almost cylindrical surface. The measurement of the surface is, however, performed along "axial" scan lines which intercept this helical path. This approach to figuring and measuring permits a relatively simple scheme to be implemented for the determination of the optimal dwell times of the figuring tool. These optimal dwell times are determined by a deconvolution which approaches the problem in a linear programming context and uses the Simplex Method. The approach maximizes the amount of material removed at any point subject to inequality constraints. The effect of using these "optimum" dwell times is to significantly improve the tools effectiveness at removing the higher spatial frequencies while staying (strictly) within the bounds and constraints imposed by the hardware. In addition, the ringing at the edges of the optic, frequently present in deconvolution problems, is completely eliminated.

Subject Terms: X-ray telescopes, grazing incidence optics, linear programming, Simplex method, deconvolution

1. INTRODUCTION

A typical x-ray telescope consists of nested shells[1-3]. Each shell is part of a long conical surface of revolution as shown in figure 1. To simplify the discussion we will assume that the part we are making is basically a cylinder. When fabricating these surfaces,

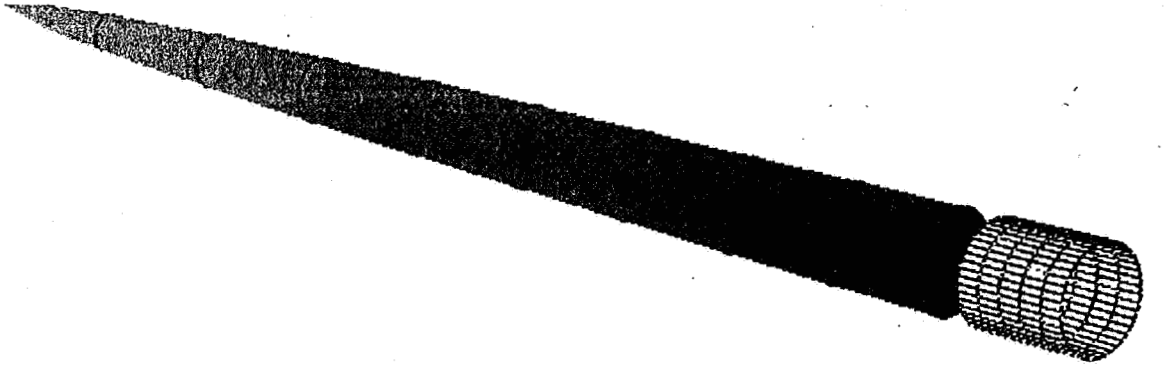

Figure 1: Conical Parent Surface and Mandrel Portion

the axis of symmetry is of course put to good use. This usually results in surfaces which have longer period surface errors azimuthally (about the axis of symmetry) and shorter period errors axially (along the axis where there is no symmetry). This is why spherical surfaces, where a symmetry about a point exists, are easier to make than aspheres. The fact that surface errors tend

to have longer periods azimuthally means that the separation of measurement points is much smaller axially, along "scan" lines, than azimuthally. This note will describe a relatively simple procedure for the considerable reduction of these axial errors by moving an abrasive (wet) grinding tool along a helical path about the cylinder. A considerable simplification results from the fact that we need only to consider one axial scan line at a time. We do not need to view the surface as two dimensional, just as a collection of one dimensional lines, one at a time. As the tool moves in its helical path and crosses each scan line the material removal is again viewed one dimensionally. This one dimensional approach reduces the amount of data needed to deconvolve dwell times and permits the determination of optimal dwell times over any scan line, one line at a time.

Optimal in our case will mean the set of dwell times determined by the Linear Programming Simplex Method [4,5] which maximizes the amount of material removed, along any scan line, subject to inequality constraints. It should be noted that without constraints maximal removal means all the material (so that one is digging holes), which is definitely not optimal and not desirable. Once the dwell times and hence the speed of the tool at each scan line crossing are determined the speed between the lines is determined by linear interpolation. The result of using these optimal dwell times is to considerably reduce the axial errors, as will be shown below.

2. GEOMETRY

The clear aperture of a x-ray optic is annular and somewhat distant from the parent optic vertex as shown in figure 1. Because of this large distance between the vertex of the parent optic and the working portion of the grazing incidence optic it is convenient to move the origin of the coordinate frame from the vertex to roughly the center of the used surface as shown in figure 2.

The equation of the surface[6] in this cylindrical coordinate frame is given by equation 1. To simplify the discussion,

$$\rho = \sqrt{\rho_0^2 + 2Kz - Pz^2} \qquad (1)$$

but, without loss of generality, we will assume that the surface is a cylinder, in which case $K=P=0$, and the equation of the surface is then just given by equation 2.

$$\rho = \rho_0 \qquad (2)$$

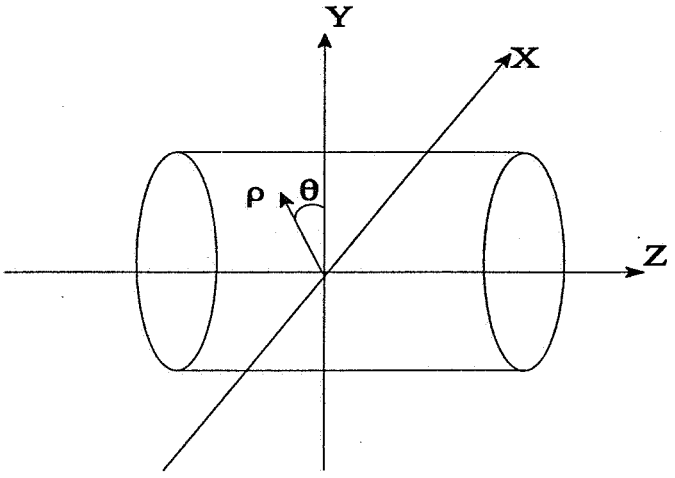

Figure 2: Body Centered Coordinate Frame

Equations 1 and 2 represent mathematically ideal surfaces. Actual surfaces will have errors or deviations (hopefully excess material), from these ideal surfaces. In the case of our cylindrical surface this will be represented by an additional (small) term as in equation 3.

$$\rho = \rho_0 + \epsilon(\theta,z) \qquad (3)$$

In the following we will assume, to simplify the discussion, that $\epsilon(\theta,z) \geq 0$ and that the desired surface is attained when $\epsilon(\theta,z) = 0$, that is we want to remove the maximum amount of excess material without digging holes.

3. SURFACE ERRORS

Determining the function $\epsilon(\theta,z)$ through measurements can be, depending on the accuracies required, not a trivial task. However difficult, the end result of all the measurements is (usually) some agreed to table of values of $\epsilon(\theta_i, z_j)$ for $i=1,...,I$ (scan line index) and $j=1,...,J$ (the axial index) and just to be specific we typically have $\theta_{i+1} - \theta_i = 10°$ and $z_{j+1} - z_j = 1\ mm$. The actual spacing and total number of data points, of course, depends on the surface knowledge requirements.

A typical scan line profile is shown in figure 3 and the goal is to reduce the error, as nearly as possible, to zero.

4. HELICAL PATH

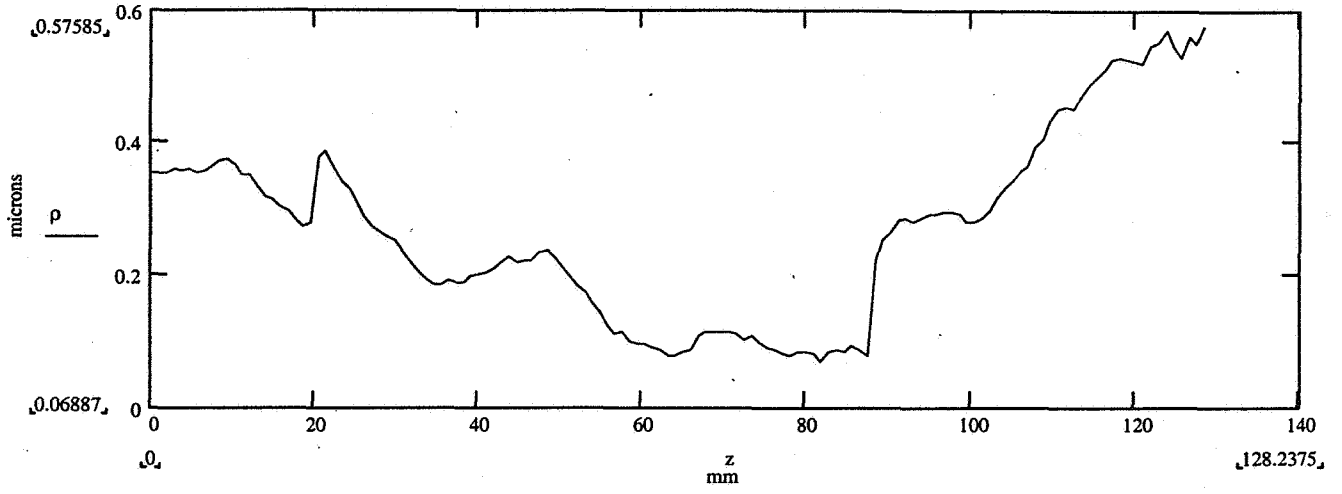

Figure 3: Axial Scan Line Profile

Reducing the figure error of our a cylinder, by moving a (wet) abrasive grinding (figuring) tool around it on a helical path is very similar to a raster pattern used for figuring "flat" optics. To see this all we need to do is imagine that we cut our cylinder along an axial scan (θ=*constant*) line and laying it flat. So that we get a rectangle, part of which is shown in figure 4.

The inclined line(s) in figure 4 is the helical path and it looks somewhat like a raster pattern. The equation of a helical path on a cylinder is given by equation 4

$$z = pitch \times \theta \ . \qquad (4)$$

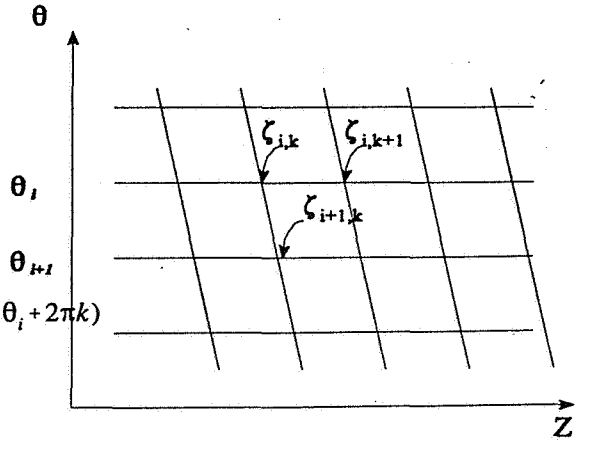

$$\zeta_{i,k} = pitch \times (\theta_i + 2\pi k) \qquad (5)$$

Figure 4: Flat Cylinder and Helical Path

The pitch of the helix is determined by (among other things) the width and shape of the tool wear profile. The helix crosses the i^{th} axial scan line at the points $\zeta_{i,k}$, given by equation 5, and where $k=1, \ldots .K$. The magnitude of K depends on the pitch of the helix and is not necessarily the same for all the scan lines. It will be at these crossing points, $\zeta_{i,k}$, that we will determine the speed, $v(\theta,z)$, of the tool along the helical path taking into account the tool wear profile and the excess material. In most of the discussion below the pitch of the

helix will be such that the tool advances one half its width, b , while going once around the cylinder. That is, the pitch in equations 4 and 5 will be $b/4\pi$.

5. ONE DIMENSIONAL TOOL WEAR FUNCTION

During a figuring operation the instantaneous material removal occurs in the small area where the tool is in contact with the part, as shown in figure 5a. The instantaneous wear is a two dimensional function. In our case determining this instantaneous removal profile with any certainty is difficult, the measured results are uncertain and consequently the use of it in material removal predictions is avoided. However, because we measure the cylinder along scan lines it is natural to determine the tool wear function, also, along scan lines as shown in figures 5a and 5b. This one dimensional characterization of the material removal is adequate for our purposes and simplifies (because we need work only in one dimension and not two) the dwell time deconvolution algorithm. In a sense, we are treating the tool as if it were moving in a "straight" line on a (cylindrical) surface at constant speed and the only quantity of interest is the amount of material removed as the tool crosses the i^{th} scan line, as shown in figures 5a and 5b.

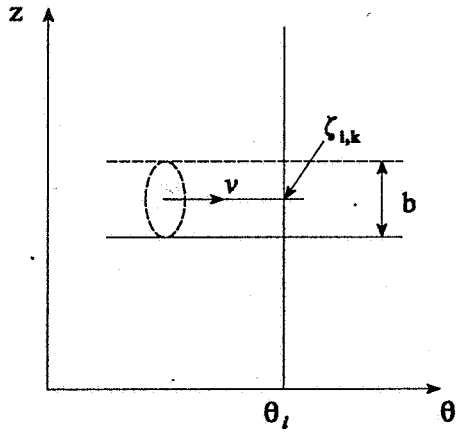

Figure 5a: Tool moving along a cylinder

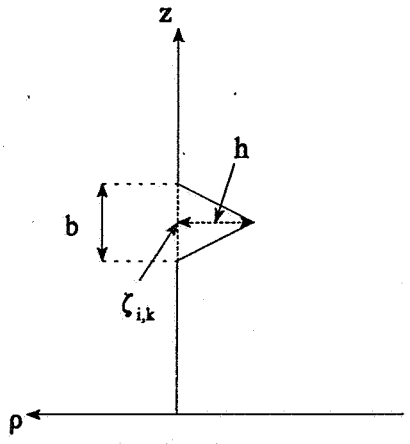

Figure 5b: Triangular material removal profile

To simplify the discussion, still further, we will assume that this one dimensional wear profile is exactly triangular in shape and given by equation 6. Here $w(z - \zeta_{i,k})$ is the material removed, along the i^{th} scan line, at the point z when the tool is at $\zeta_{i,k}$ and where b is the base and h/v is the height of the triangle which is inversely proportional to the speed, v, of the tool along its path. The constant, h, is a measured quantity and is the depth of wear for a unit speed.

$$w(z-\zeta_{i,k})=\begin{bmatrix} -\frac{2h}{v}\frac{|z-\zeta_{i,k}|}{b} & for\ |z-\zeta_{i,k}| \le \frac{b}{2} \\ 0 & for\ |z-\zeta_{i,k}| > \frac{b}{2} \end{bmatrix} \qquad (6)$$

The wear, $w_i(z)$, at any point z , along the i^{th} scan line from all of the (helical path) tool positions is given by equation 7

$$w_i(z) = \sum_{k=1}^{K} h_k w(z-\zeta_{i,k}) \quad . \qquad (7)$$

Figure 6 shows the wear pattern, along the i^{th} scan line when $v=1$ and when the pitch of the helix is such that $\zeta_{i,k} - \zeta_{i,k+1} = b/2$.

We see, in this case, that the material removal is (except for edge effects) just a uniform lowering of the surface, $\Delta\rho=h$.

Now, another quantity that will be of interest is the total wear, W, along the i^{th} scan line given by equation 8 where the

$$W_i = \sum_{j=1}^{J} w_i(z_j)\Delta z = \sum_{j=1}^{J}\sum_{k=1}^{K} h_k w(z_j-\zeta_{i,k})\Delta z \qquad (8)$$

summation is over all of the (equispaced Δz) data points, z_j ,on a scan line. Equation 8 is just the total height reduction in a θ_i=*constant* plane. In the case of a cylinder (ρ=*constant*) the volume of material removed in an angularly thin wedge , $\delta\theta$, is then just $W\rho\delta\theta$. Again, figure 6 shows the removal along a scan line for three tool positions when all the h_k are constant.

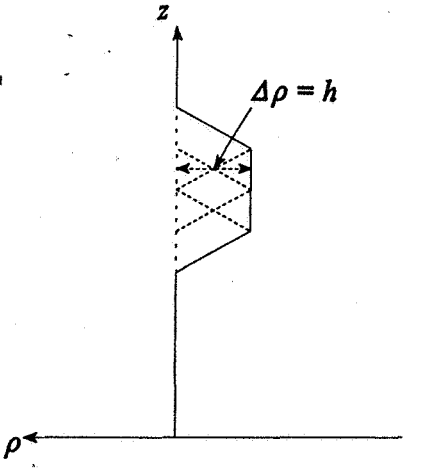

Figure 6: Uniform removal

An objective of a figuring operation is to vary the removal, by varying the h_k , in such a way that we remove the maximum amount of material, but not "dig holes" by going below the desired surface. This maximum value of W can be found by means of the Linear Programming Simplex Method as described in the next section.

6. MAXIMIZING THE TOTAL WEAR BY THE SIMPLEX METHOD

The Linear Programming Simplex Method finds the maximum or minimum value of a linear functions taking into account inequality constraints. In our case, we want to find the values (for a given scan line, hence we drop the subscript i)

$$h_k \quad for \quad k=1\ldots K$$

which maximize the function W , given by equation 8

$$W = \sum_{j=1}^{J} w(z_j) = \sum_{j=1}^{J}\sum_{k=1}^{K} h_k w(z_j-\zeta_k) \qquad (8)$$

subject to the, J, inequality constraints, given by equation 9, of not digging holes

$$w(z_j) \le \epsilon(\theta,z_j) \quad for \quad j=1\ldots J \qquad (9)$$

and any additional constraints, given by equation 10, on the dwell times, which here are constraints on the heights of the triangles.

$$h_k^{min} \le h_k \le h_k^{max} \quad for \quad k=1\ldots K \qquad (10)$$

Again, we have dropped the scan line index, i , as we are discussing only one scan line at a time.

7. OPTIMIZATION RESULTS - DECONVOLUTION EXAMPLE

Figure 7 shows the results on this Simplex Method dwell time deconvolution applied to the axial scan profile shown in figure 3. The tool wear is triangular, the tool spacing is, *b/2* , one half the base of the triangle. The varying heights of the triangles are proportional to the dwell times. The amount of material removed at any tool position is equal to the area under the triangle. The tool, centered at the 93 mm point has a height of zero and none of the removals are negative. The predicted new surface is shown

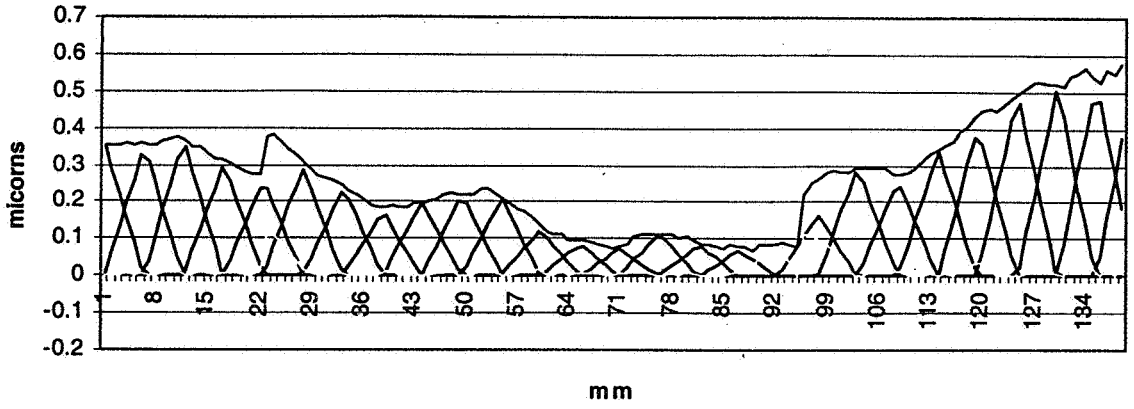

Figure 7: triangular tool positions and wear heights

in figure 8 as the bottom dashed curve. It should be noted that the amount of material removed never exceeds, because of the inequality constraints, the original residual $\epsilon(\theta_i, z_j)$.

8. FOURIER ANALYSIS OF SCAN LINE

Equations 10 and 11 connect the scan line profiles, in figure 8, with the respective Fourier coefficients

$$\epsilon(z_j) = A_0 + \sum_{n=1}^{N_f}\left[A_n\cos\left(2\pi n\frac{j}{J}\right) + B_n\sin\left(2\pi n\frac{j}{J}\right)\right] \quad (10)$$

$$\epsilon(z_j) - \sum_{k=1}^{K} h_k w(z_j-\zeta_k) = a_0 + \sum_{n=1}^{N_f}\left[a_n\cos\left(2\pi n\frac{j}{J}\right) + b_n\sin\left(2\pi n\frac{j}{J}\right)\right] \quad (11)$$

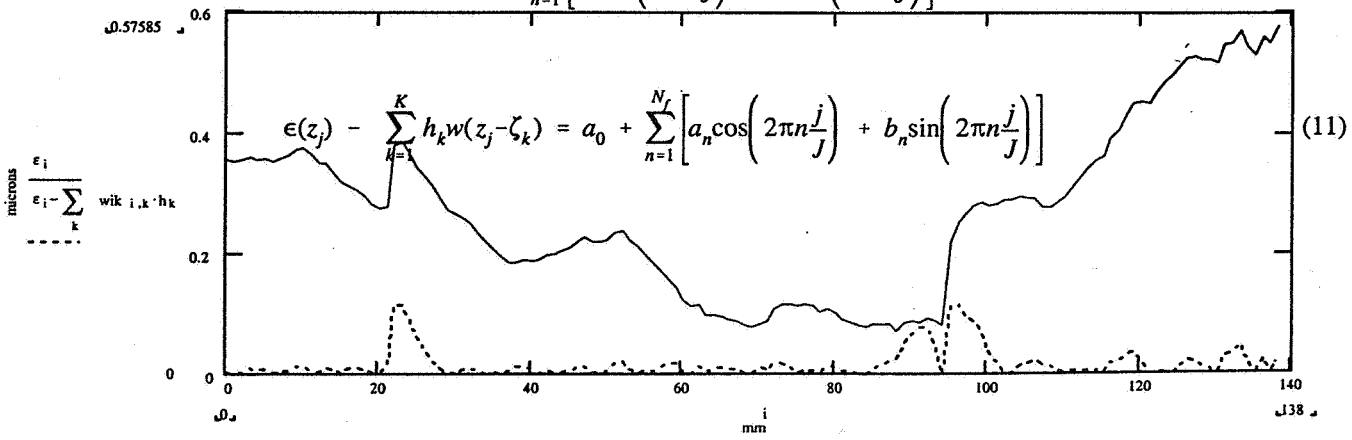

Figure 8: Original and new residual

where J is the total number data points and N_f= integer portion of $J/2$. Plotting the (un-normalized) power spectrum of the coefficients of each curve, as in figure 9, we see that the coefficients, in equation 11, are reduced out to slightly beyond $n=10$ or a spacial wavelength of about 10mm which is the width, b, of the triangular tool in this example.

9. SPEED BETWEEN SCAN LINES

Once we have determined the speed, $v_{i,k}$, of the tool at each scan line and helix crossing point we find the tool speed, v, between two consecutive scan line crossings by linear interpolation as in equation 13

$$v = \frac{\Delta v}{\Delta s} s + v_{i,k} \tag{13}$$

Where $\Delta v = v_{i+1,k} - v_{i,k}$ is the change in speed, Δs is the path length between two consecutive crossings. s and $v_{i,k}$ is the path length and speed, respectively, from the last crossing.

10. CONCLUSION

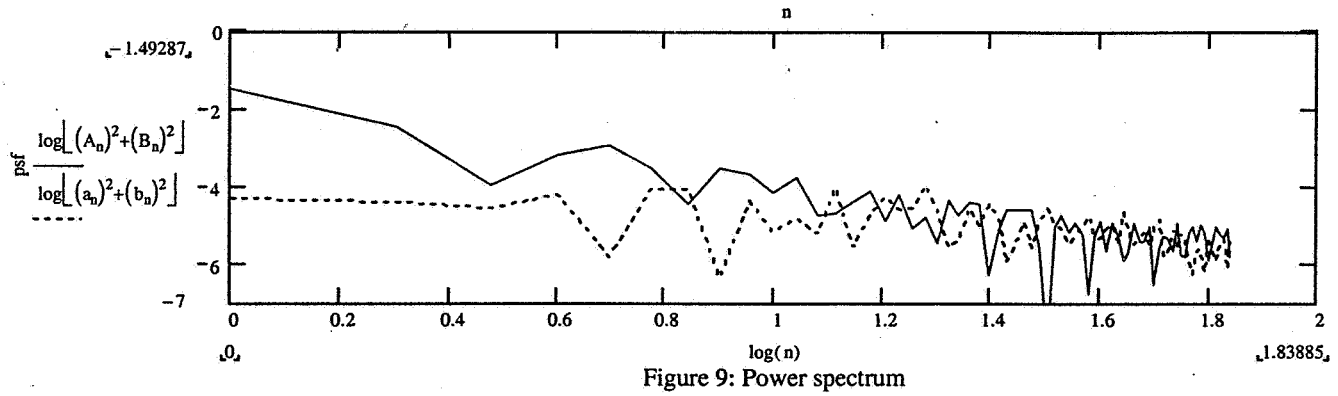

Figure 9: Power spectrum

The end result of all of these operations is that we have determined the speed of motion of a figuring tool along a helical path and the speed is optimum at the scan line crossings. It should be noted that approach is very similar to the technique[7,8] used to determine the optimum dwell times for the polishing and figuring of the AXAF, now called Chandra, cylindrical optics. In the case of the Constellation-X mandrels it is hoped that this approach also improves the convergence of the figuring process.

Deconvolution methods which attempt to reduce the rms deviation directly are simply solving sets of overdetermined linear equations for the unknown dwell times. This "traditional" approach certainly works very well when there are no constraints on the dwell times. However, even with the simple requirement that all dwell times be positive significantly, complicates finding an optimum solution. Other constraints further complicate the numerical search for the best solution.

The Simplex, linear programming, approach is an alternative method for determining dwell times. This approach seeks to determine a set of dwell times which maximize the amount of material to be removed but, of course, subject to constraints. Its major advantage, is numerical stability, reduction in rms surface roughness which is comparable to or better than the direct rms reduction approach and a certain intuitive appeal.

ACKNOWLEDGMENTS

The development of the above algorithm is not a product of inspiration but of dogged work (at the then Perkin-Elmer Corporation) in support of the manufacture of (large) optics. It is in that setting that one is forced to seek optimum approaches to every step of a process as the alternatives are more costly. However it should be noted that (way back) just prior to the start of the AXAF polishing work the availability of the NIST FORTRAN computational libraries[9] considerably simplified and made possible this particular, Simplex, approach. Now, the task is made still easier with the help of Mathcad™.

Of course thanks go to Hughes Danbury Optical Systems (HDOS a.k.a. Perkin-Elmer) where the original development work occurred funded by various NASA contracts. The current work was performed at NASA and supported by the Constellation-X Soft X-ray Technology Program and the Cross Enterprise Technology Development Program.

REFERENCES

1. See the description of Constellation-X online at: http://constellation.gsfc.nasa.gov/booklet/toc.html.

2. D. Content, T. Saha, R. Petre, J.J. Lyons III, G. Wright, J. Zaniewski, K.W. Chan, "Superpolishing and Precision Metrology on a Metal Mandrel and Replicated Segments for Constellation-X", Proc. SPIE, **3766**, 22, 1999.

3. R. Petre, C. Chen, L. Cohen, D. Content, R.J. Harms, O. Mongrard, G. Monnelly, T. Saha, M. Schattenburg, P. Serlemitsos, and W. Zhang, "Segmented x-ray mirror development for Constellation-X", Proc. SPIE, **3766**, 11, 1999.

4. G. Hadley, Linear Programming. Reading, Mass.: Addison-Wesley, 1961.

5. A.P. Bogdanov, "Optimizing the technological process of automated grinding and polishing of high-precision large optical elements with a small tool", Soviet Journal of Optical Technology, Vol. 52(7).

6. R.J. Noll, P.E. Glenn, J. Osantowski, "Optical surface analysis code (OSAC)", Proc. SPIE **362**, 78-85, 1983.

7. J.R. Johnson, E. Waluschka, "Optical Fabrication - Process Modeling - Analysis Tool Box", Proc. SPIE **1333**, 106, 1990

8. P.B. Reid, "Fabrication and predicted performance of the Advanced X-ray Astrophysics Facility mirror ensemble", Proc. SPIE 2515, 361, 1995

9. Now available at http://gams.nist.gov/serve.cgi/Module/CMLIB/SPLP/2055